IEEE Access
Multidisciplinary | Rapid Review | Open Access Journal

Received July 14, 2020, accepted July 24, 2020, date of publication July 29, 2020, date of current version August 10, 2020.

Digital Object Identifier 10.1109/ACCESS.2020.3012633

Hybrid Grey Wolf Optimizer for Transformer Fault Diagnosis Using Dissolved Gases Considering Uncertainty in Measurements

AYMAN HOBALLAH[1,2], DIAA-ELDIN A. MANSOUR[2], (Senior Member, IEEE), AND IBRAHIM B. M. TAHA[1,2]

[1]Electrical Engineering Department, College of Engineering, Taif University, Taif 21974, Saudi Arabia
[2]Electrical Power and Machines Department, Faculty of Engineering, Tanta University, Tanta 31521, Egypt

Corresponding author: Ayman Hoballah (ayman.hoballah@f-eng.tanta.edu.eg)

ABSTRACT The transformer fault diagnosis based on dissolved gas analysis is greatly affected by the uncertainties existing in measured data during oil sampling, handling and storage. This work aims to develop an efficient code matrix based on dissolved gas percentages for accurate fault diagnosis considering measurement uncertainties. Fuzzy system is utilized to produce the rules that map the limits of gas ratios for different fault types. Each gas percentage range is divided into three regions represented by three fuzzy memberships. The fuzzy system is then developed to relate the gas percentages to the fault type. The membership limits are then optimized by using heuristic algorithms in order to maximize the accuracy. Hybrid Grey Wolf Optimization (HGWO) algorithm is utilized to produce the diagnostic code matrix. The proposed code limits the impact of measurement uncertainties on the output fault diagnosis. Different levels of measurement uncertainties up to 20% are considered to validate the effectiveness of the new code in improving the diagnostic accuracy. The accuracies during the training and testing processes attained 97.45% and 95.45%, respectively, with the maximum uncertainty level of 20%. Moreover, randomly selected case studies representing various fault types are investigated using the proposed method. For each case study, various levels of uncertainties are imposed on the original data. The proposed method proved its easiness towards diagnosing transformer faults and robustness against measurement uncertainties.

INDEX TERMS Power transformers, dissolved gas analysis, heuristic algorithms, fuzzy systems, measurement uncertainty.

I. INTRODUCTION

Power transformers represent the vital power system equipment. The accurate diagnostic accuracy of transformer faults is an important topic for power system reliability and continuity. The early detection of transformer faults is beneficial in planning the maintenance schedule and avoiding unscheduled load curtailment and fire hazards. Nowadays, transformers operate near their full capacity due to rapid increase of load demand. This leads to an increase in the electrical, thermal and chemical stresses on the transformer insulation [1], [2]. The stresses can incept faults inside the transformer such as overheating, partial discharge, and arcing. Lack of proper diagnosis of these faults can cause severe damage and eventual failure of the transformer. Therefore, several methods were proposed for accurate fault diagnosis in transformers based on the analysis of insulating oil. Dissolved gas analysis (DGA) is the most used method for fault diagnosis [3], [4]. DGA is based on the correlation between dissolved gases in the oil and corresponding fault type and severity. The most common faults in transformers are classified into six types that are partial discharge (PD), low energy discharge (D1), high energy discharge (D2), low temperature fault (T1), medium temperature fault (T2), and high temperature fault (T3). The most common dissolved gases generated under these faults are five combustible gases; hydrogen (H_2), methane (CH_4), ethane (C_2H_6), ethylene (C_2H_4) and acetylene (C_2H_2). In addition, there are two other gases responsible for diagnosing degradation of cellulose insulation. These gases are carbon monoxide and carbon dioxide. Since cellulose degradation is specific in its gas generation, it can be dealt separately by diagnostic methods.

The associate editor coordinating the review of this manuscript and approving it for publication was Diego Oliva.

Many conventional methods were proposed to identify the transformer faults based on DGA such as key gas method [1], ratio methods [5]–[7], and graphical methods [8]–[12]. Some of these methods were targeting diagnosis of main fault types in transformer oil and others were developed to include cellulose degradation. These conventional methods are limited in their diagnostic accuracy.

Artificial intelligent methods were widely used to develop DGA based diagnosis with high accuracy. The first example of these methods was the artificial neural network (ANN), in which much training data were used to adapt the network for DGA diagnosis [13]–[16]. The input for ANN can be fuzzified gas concentrations [13], certain gas ratios [14]–[16], or others [16], [17]. The second example of artificial intelligent methods is the fuzzy logic system, in which several If-Then rules were implemented to correlate DGA with the proper diagnosis [18]–[20]. Also, support vector machine (SVM) was proposed as an example of artificial intelligent methods with a slight increase in the diagnostic accuracy compared to others [21]–[23]. In addition, other artificial intelligent methods have been introduced to increase the diagnostic accuracy such as adaptive neural fuzzy inference system [24], gene expression programming approach [25], and Bayesian networks [26].

The uncertainties and noises in measured DGA data affect strongly the ability of DGA methods on transformer fault diagnosis. In most methods, the diagnostic accuracy depends on the numeric limits and the boundaries of gas contents within DGA data. Therefore, uncertainties associated with measured data may lead to serious deterioration in diagnostic accuracy, and consequently, these uncertainties should be considered during the evaluation process of the diagnostic method. In [27], two SVM based algorithms were developed using fuzzy c-means clustering and kernel fuzzy c-means clustering methods to consider the possible noises, outliers and imbalances in measurements without producing clear curing code or numeric validation. In addition, the technique developed in [27] needs special programing, making it impractical for the engineers at transformer stations. Thus, more investigations are required to develop clear and robust methodology for accounting such uncertainties in measurements.

This work aims to develop DGA based diagnostic method robust against measurement uncertainties using fuzzy logic system and heuristic optimization techniques. The main target is to create a tabulated code that relates the percentages of dissolved gases having different levels of measurement uncertainties to the fault type.

The problem is formulated as a constrained optimization problem that need to be solved using heuristic optimization (HO) techniques. Hybrid Grey Wolf Optimizer (HGWO) technique was used to attain the global solution fast that achieves the best diagnostic accuracy. The fuzzy system is used to relate the actual percentages of gases with the fault types utilizing the membership functions for various percentages and the corresponding diagnostic rules. Then, HGWO technique is used to specify the division limits of gas percentages and the fault type aiming to maximize the diagnostic accuracy. Genetic Algorithm (GA) and Particle Swarm Optimization (PSO) was also used to validate that the obtained solution is the global one.

A 407 datasets are used to test the proposed method. These datasets were collected from Egyptian Electricity Utility and literatures [28]–[31]. The obtained code is implemented considering different degrees of uncertainties in the collected datasets, 5%, 10%, 15%, and 20%. The optimal limits of gas percentages are converted into code tree that can be easily used to specify the fault type. The results of the proposed method were compared to other methods to validate its robustness against uncertainty.

II. UNCERTAINTY AND RESEARCH MOTIVATION

DGA based diagnostic methods of transformer faults are strongly affected by the exact measurement and analysis of dissolved gases. Currently, the most adopted DGA process is the offline one, which is composed of three main procedures. The first procedure is extracting the oil sample from the considered transformer. The second procedure is separating the gas phases of the oil. The third and last procedure is diagnosing the fault type by any relevant method. Oil sampling is carried out using special syringes. Then, samples are stored and transferred to the laboratory for testing. During storage and transfer, many factors affect gas concentrations such as temperature and storage time. Several techniques were used for gas separation. The most critical factor that affects gas concentrations during separation is the air bubbles. The existence of air bubbles causes a significant reduction in dissolved gases due to the diffusion of gases into the air bubble and leaving the oil [32]. All these factors act towards increasing uncertainties in input gas concentrations and reducing diagnostic accuracy. So, it is important to consider these factors in developing any DGA based diagnostic method. According to [33], the storage and temperature can cause uncertainties up to $\pm 14\%$ and uncertainties due to measurement accuracy are within $\pm 5\%$. Accordingly, overall uncertainties in DGA data can be considered as $\pm 20\%$.

Regarding conventional DGA methods, they have already limited accuracy. So, any further decrement in the accuracy due to uncertainties in the input data will make these methods unpractical. For ANN, SVM, or any similar methods, they tend to be a black box adapted for certain dataset. Accordingly, they lack a proper representation of uncertainties. For fuzzy logic, it can accommodate a proper infrastructure for dealing with uncertainties if proper membership functions have been built and enough rules has been implemented [34], [35]. To the best of our knowledge, none of the previous DGA diagnostic methods considered uncertainties in their implementation.

III. PROPOSED METHOD

As discussed above, the fuzzy logic system can deal effectively with uncertainties in input data if proper membership

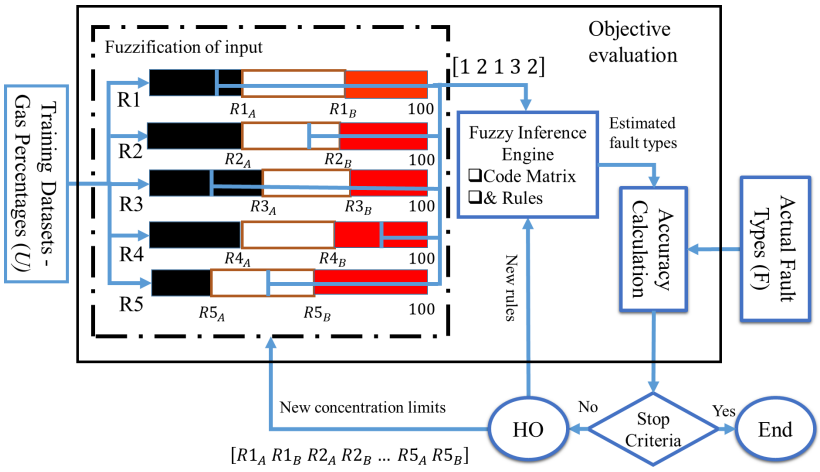

FIGURE 1. The proposed algorithm for new code preparation.

functions have been built and sufficient number of rules has been implemented. Accordingly, the main structure of the proposed method is built based on the fuzzy logic system. Percentages of the dissolved gas concentrations vector (**R**) in each dataset are used as input indices for predicting the corresponding fault types (**F**) as follows:

$$\mathbf{R} = \begin{bmatrix} \mathrm{R1} \\ \mathrm{R2} \\ \mathrm{R3} \\ \mathrm{R4} \\ \mathrm{R5} \end{bmatrix} = 100 \times \begin{bmatrix} \mathrm{H_2/TCG} \\ \mathrm{CH_4/TCG} \\ \mathrm{C_2H_6/TCG} \\ \mathrm{C_2H_4/TCG} \\ \mathrm{C_2H_2/TCG} \end{bmatrix} \quad (1)$$

$$\mathrm{TCG} = \mathrm{H_2} + \mathrm{CH_4} + \mathrm{C_2H_6} + \mathrm{C_2H_4} + \mathrm{C_2H_2} \quad (2)$$

where, TCG is the total amount of dissolved combustible gases in the transformer oil.

The first stage towards limiting the impact of uncertainties is the use of the percentage gas, where uncertainty value becomes normalized by the overall concentration of the total combustible gases. Different uncertainty levels were randomly assumed in the input data up to 20% as declared in the previous section. The uncertainty was generated by applying a random error or noise vector to the original vector [36]. The percentage error (E) can be expressed as follows:

$$E = x \times r \quad (3)$$

where r is a random vector ranging between 0 and 1 and x is the required step of uncertainty levels, which is taken as 5% in this study. This error is then added to an offset K to increase the uncertainty level. As an example, if K is specified as 10%, the total uncertainty level after adding E will be 15%. Different degrees of uncertainties in the collected datasets are implemented in this study ranging between 5% and 20% with a step of 5%. Based on the error vector in (3), a new vector of uncertain data (U) is created as follows [37]:

$$U = [1 \pm (E + K)] \times R \quad (4)$$

The original and modified data were combined together to form the input data to the proposed methodology. The five gas percentage values were used to specify the fault type. The proposed code was obtained by dividing each gas percentage into three regions (three memberships) with the corresponding two limits between 0% and 100% as shown in Fig. 1. Therefore, considering the five gas percentages and the limits of each gas percentage (0, R_A, R_B, 100), the membership limits matrix (R_L) can be written as follows:

$$R_L = \begin{bmatrix} 0 & R1_A & R1_B & 100 \\ 0 & R2_A & R2_B & 100 \\ 0 & R3_A & R3_B & 100 \\ 0 & R4_A & R4_B & 100 \\ 0 & R5_A & R5_B & 100 \end{bmatrix} \quad (5)$$

The five gas percentages with three ranges create 243 different rules which were used to build the membership functions of the fuzzy system. These rules represent the initial overall code matrix during the optimization process. Using this large number of rules is intended to cover different possibilities of input-output combinations. Then, the datasets were processed using the fuzzy logic system to estimate the fault type, by representing the different regions of each gas concentration using membership functions. The fuzzification process is the second stage towards limiting uncertainties, where there will be a small shift in fuzzified value after uncertainty. So, any violation of a certain rule due to uncertainty will be compensated by other rules. Finally, HGWO was used for optimizing the limits of membership functions and the fault type corresponding to each rule aiming to maximize the diagnostic accuracy considering both original data and uncertain ones. GA and PSO algorithms were also used to guarantee attaining the optimal solution.

The main steps of the proposed algorithm are presented in Fig. 1. They contain three main processes as follow:

A. The original datasets were collected, and new datasets were created based on the expected random uncertainty

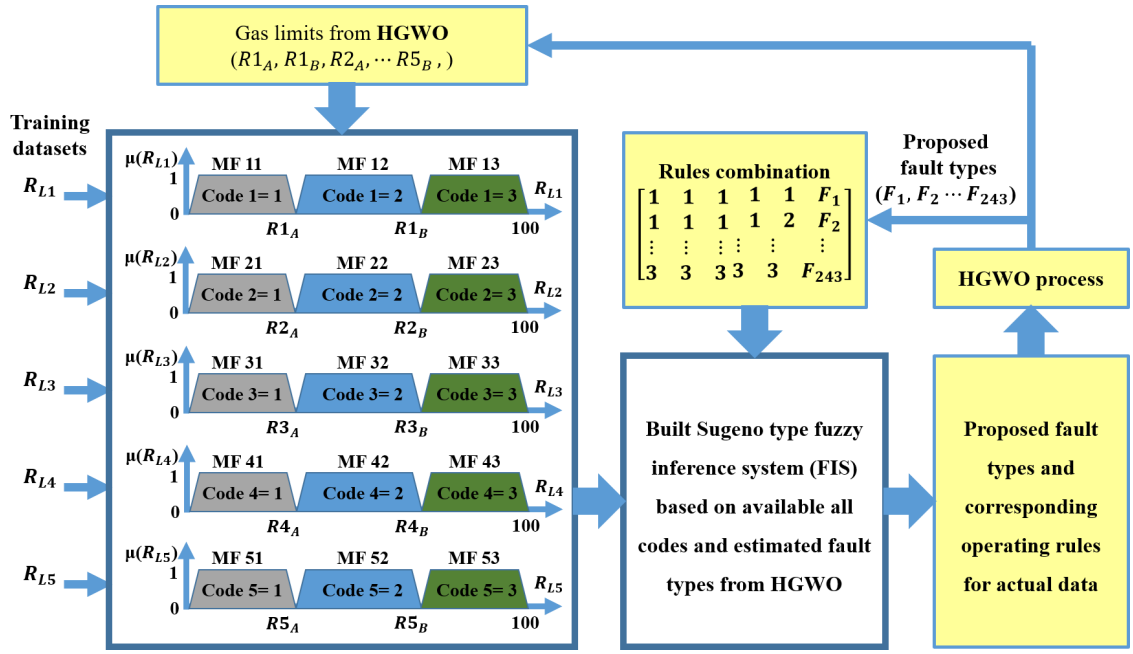

FIGURE 2. Schematic diagram for fuzzy inference system.

in the gas concentrations by using (4). Furthermore, the percentages of the dissolved gas concentrations were calculated in each set.

B. Sugeno type fuzzy inference system (FIS) was used to relate the dissolved gas percentages and the fault types through set of rules which covering all available combinations of membership functions with the limits specified in Equation (5). HGWO was used to continuously update the FIS by modifying the membership limits and fault types corresponding to each rule in the direction of diagnostic accuracy maximization. Therefore, the actual percentages of the dissolved gas concentrations (inputs) are used to determine the code matrix (rules) based on the membership function limits, which were provided from the HGWO as shown in Fig. 2. The fault types are marked 1, 2, 3, 4, 5 and 6 to represent the fault types PD, D1, D2, T1, T2, and T3, respectively.

C. The objective function (Accuracy) was calculated using the percentage of the number of true estimated fault types by the proposed model (N_{true}) and the total number of samples (N_{all}). The sum of the width of membership functions of each gas percentage must be 100. The optimal limits of gas percentages were specified by using the optimization process.

IV. OPTIMIZATION ALGORITHMS

The problem was formulated as a constrained objective function. Three optimization algorithms were used to obtain the optimal gas percentage limits, thereby formulating the code tree for accurate fault diagnosis. The fitness function was the diagnostic accuracy.

Maximize :

$$f(x) = 100 \times N_{true}/N_{all} \tag{6}$$

Subject to :

$$Ri_A \leq Ri_B \leq 100 \quad i = 1, 2, \ldots 5 \tag{7}$$

A. THE BASIC GREY WOLF OPTIMIZER (GWO)

GWO is a population based optimization algorithm which simulates the social behavior of grey wolves [38]. Equations (8) to (15) present the mathematical model which includes the hunting process based on the best three positions of grey wolves $(x_\alpha, x_\beta, x_\delta)$. Random search behavior was used to avoid falling into local minimum position by decreasing the parameter $a_{(.)}$ from 2 to 0. In the current study, each individual represents the membership matrix limits (R_L) in (5) and the fault types corresponding to all 243 rules described in Fig. 2.

$$x^{k+1} = (x_1 + x_2 + x_3)/3 \tag{8}$$

$$x_1 = x_\alpha - a_1 d_\alpha \tag{9}$$

$$x_2 = x_\beta - a_2 d_\beta \tag{10}$$

$$x_3 = x_\delta - a_3 d_\delta \tag{11}$$

$$d_\alpha = \left| c_1 x_\alpha - x^k \right| \tag{12}$$

$$d_\beta = \left| c_2 x_\beta - x^k \right| \tag{13}$$

$$d_\delta = \left| c_3 x_\delta - x^k \right| \tag{14}$$

$$a_{(.)} = 2lr_1 - l, c_{(.)} = 2r_2 \tag{15}$$

where x_α, x_β, and x_δ are the most three fittest positions of the prey in the k iteration, x_1, x_2 and x_3 are the modified positions of the grey wolf, l is decreased from 2 to 0, and r_1 and r_2 are random numbers between 0 and 1.

The basic GWO failed to catch the optimal solution where the simulation was settled frequently at a local minimum solution. Therefore, the algorithm was modified to enhance the ability of GWO to settle at the optimal solution. Several methods have been used to improve the convergence performance of the GWO [39]. Modifications were applied to improve the ability of GWO to discover the search area and converge at the optimal solution.

B. HYBRID GREY WOLF OPTIMIZER (HGWO)

HGWO with GA was developed to improve the exploration, the exploitation and diversity [39]–[43]. In this work, additional loop of PSO was added to keep the gained experience of the HGWO with GA by memorizing the local best positions and global best position [30]. The individuals modify their positions using the velocity (v^{k+1}) based on the distance between the position of individuals, their local best positions (x_{lb}^k) and global best position (x_α). The best three positions of grey wolfs are then memorized to be used in the next GA loop.

$$x^{k+1} = x^{k+1} + \chi v^{k+1} \tag{16}$$

$$v^{k+1} = wv^k + Ar_3\left(x_{lb}^k - x^{k+1}\right) + Br_4\left(x_\alpha - x^{k+1}\right) \tag{17}$$

$$w = w_{max} - (w_{max} - w_{min}) \times (k/max.Iteration) \tag{18}$$

where A and B are constant between 1.2 and 2, r_3 and r_4 are random numbers between 0 and 1, and χ is a construction factor to control the diversity.

GA is a heuristic iterative optimization technique which tends to modify the individuals based on the selection, crossover and mutation processes using (19) and (20) [5], [44]. Fittest individuals (parents) were used to generate new solutions (offsprings). The better individuals survive and represent new parents for the next iteration. The GA mechanism was applied on the local best positions gained by PSO individuals to keep diversity and discover new search areas around the best solution. The target is to modify x_α,x_β, and x_δ to improve the ability of the GWO to obtain the optimal solution [45].

$$x_{ij}^{k+1} = x_{lj}^k \tag{19}$$

$$x_{ij}^{k+1} = x_{ij}^k + \gamma*(x_{ij}^{max} - x_{ij}^{min}) \tag{20}$$

$$\boldsymbol{x} = \begin{bmatrix} R1_A & R1_B & \cdots & R5_B & F_1 & \cdots & F_{243} \end{bmatrix} \tag{21}$$

where γ is a random generated number between 0 and 1, $\boldsymbol{x}$ is the vector of variables, x_{ij}^{max} and x_{ij}^{min} are the maximum and minimum limits, $R1_A$ to $R5_B$ are the gas percentage limits, and F_1 to F_{243} are the proposed fault types for all rules.

The pseudo code of the hybrid GWO is described as follows:

Algorithm 1 Hybrid Grey Wolf Optimizer Algorithm

Initialize GWO, PSO and GA parameters
Initialize the population $X(i = 1, 2 \ldots n)$ *of the HGWO*
Calculate the individual fitness values by (5)
Record the best three individuals (x_α, x_β,x_δ)
While ($t <$ *maximum iteration number)*
Update the position of all individuals of PSO by (15)
Check the variable limits
Calculate the fitness value of individuals by (5)
Update the best three individuals (x_α, x_β,x_δ)
Modify the position of GA individuals by (18)-(19)
Check the variable limits
Calculate the fitness values by (5)
Update the best three individuals (x_α, x_β,x_δ)
Update the position of GWO individuals by (7)-(14)
Check the variable limits
Calculate the fitness values by (5)
Update the best three individuals (x_α, x_β,x_δ)
Check the satisfaction of stopping criteria
$t = t + 1$
Update a, c, d
End While
Return the best individual, x_α,

TABLE 1. Parameters of HGWO.

No. of variables	253	Crossover Percentage	0.5
wmax	0.98	Mutation Rate	0.05
wmin	0.4	Mutation Percentage	0.5
A	1.8	Mutation operator	Random
B	1.8	Crossover operator	Two points
Constraints	10	Number of Offsprings	60

V. CODE IMPLEMENTATION

The new codes for transformer fault diagnostics were prepared using the membership limits obtained from the optimization process. The parameters of HGWO, PSO, and GA with 30 population and 2000 maximum iterations are presented in Table 1.

The collected data were shuffled and randomly divided into 75% to perform the optimization process and the remaining 25% are used for testing purposes. The variables are the 10 membership limits as in (5) and the fault types corresponding to all possible 243 fuzzy rules which were obtained from the combination of the five gas percentages with three memberships. Each of the five gas percentages had three codes [1, 2, 3] based on the limits from zero to 100% as shown in Fig. 2. The available 243 rules start from [1 1 1 1 1], [1 1 1 1 2], [1 1 1 1 3] to [3 3 3 3 3]. The target is to specify the variables that maximize the accuracy of fault diagnosis. Among these 243 rules, there will be operating fuzzy rules resulted from the optimization process based on the correct allocation of input data (gas percentages) and actual fault types.

TABLE 2. The diagnostic accuracy of the GWO and HGWO algorithms.

Data sets	GWO	HGWO
Train data	95.62	97.45
Test data	91.68	95.45
All data	94.64	96.95
0 % Uncertainty degree	96.31	100
5 % Uncertainty degree	96.56	98.77
10 % Uncertainty degree	95.58	98.03
15 % Uncertainty degree	92.87	95.09
20 % Uncertainty degree	91.89	93.12

TABLE 3. The gas percentages coding and limits.

Gas percentage	Membership limits	Code
R1	$0 < R1 \leq 31.68$	C1=1
	$31.68 < R1 \leq 51.62$	C1=2
	$51.62 < R1 \leq 100$	C1=3
R2	$0 < R2 \leq 55.00$	C2=1
	$55.00 < R2 \leq 80.55$	C2=2
	$80.55 < R2 \leq 100$	C2=3
R3	$0 < R3 \leq 18.09$	C3=1
	$18.09 < R3 \leq 24.98$	C3=2
	$24.98 < R3 \leq 100$	C3=3
R4	$0 < R4 \leq 10.54$	C4=1
	$10.45 < R4 \leq 40.00$	C4=2
	$40.00 < R4 \leq 100$	C4=3
R5	$0 < R5 \leq 2.45$	C5=1
	$02.45 < R5 \leq 76.69$	C5=2
	$76.69 < R5 \leq 100$	C5=3

The optimization process was repeated many times using HGWO and basic GWO. The results validated the ability of HGWO to obtain the optimal solution each time. On the other hand, basic GWO is settled at different local minima due to the large number of variables in the problem under investigation which combined continues variables (membership limits) and discrete ones (fault types). Table 2 presents the diagnostic accuracy of the basic GWO and HGWO optimization algorithms. The results illustrate the effectiveness of HGWO to detect the transformer fault types with different uncertainty levels compared to the basic GWO.

The optimization process was carried out many times using HGWO, GA, and PSO. Each time, HGWO proved not only to catch the optimal solution but also to be the fastest algorithm. The same optimal solution was obtained by using the three optimization techniques with the same diagnostic accuracy. Equation (22) presents the obtained optimal limits of gas percentages and Table 3 presents the corresponding ranges of the membership functions.

$$R_L = \begin{bmatrix} 0 & 31.68 & 51.62 & 100 \\ 0 & 55.00 & 80.55 & 100 \\ 0 & 18.09 & 24.98 & 100 \\ 0 & 10.45 & 40.00 & 100 \\ 0 & 02.45 & 76.69 & 100 \end{bmatrix} \quad (22)$$

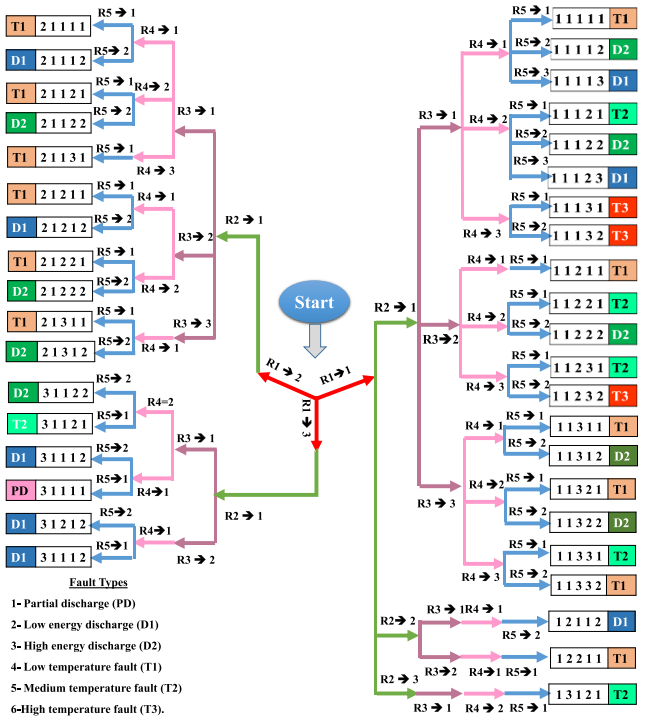

FIGURE 3. Developed code tree formulation.

After optimization process, the operating rules became 39 rules formed in a code tree to specify the fault types in relation to the five percentages of dissolved gas concentrations as shown in Fig. 3. The use of the code tree starts with determining the code of R1 towards R5 based on the membership limits at Table 3 and ends by the corresponding expected fault type expressed as a code matrix. The overall fault diagnostic accuracy of the optimal solution was 96.95% considering both training and testing datasets. By analyzing the code tree, the allocation of fault types with the actual data without uncertainties belongs to 34 branches which covers all fault types. This means that 5 fuzzy operating rules became operative to account for the uncertainty in measurements.

As a case study to illustrate step by step the usage of the code tree, a sample of data was used with five gas values of 37800, 1740, 249, 8 and 8 corresponding to H_2, CH_4, C_2H_6, C_2H_4 and C_2H_2, respectively. The total dissolved gas contents were 39805. The percentages of gases are 94.96%, 4.37%, 0.625%, 0.02% and 0.02%, which, representing R1, R2, R3, R4 and R5, respectively. The fault diagnostic starts with creating the code matrix corresponding to gas percentages according to the limits in Table 3. The code matrix is [3 1 1 1 1] based on the membership limits. By tracking the branch in the code tree starting from R1 at 3, R2 at 1, R3 at 1, R4 at 1 and R5 at 1, the branch ended by the corresponding fault type that can be easily found as partial discharge (PD) as shown in Fig. 4. This can be visualized by the rule viewer of FIS depicted in Fig. 5. The code tree formulation can be easily used by relevant engineers without any complicated

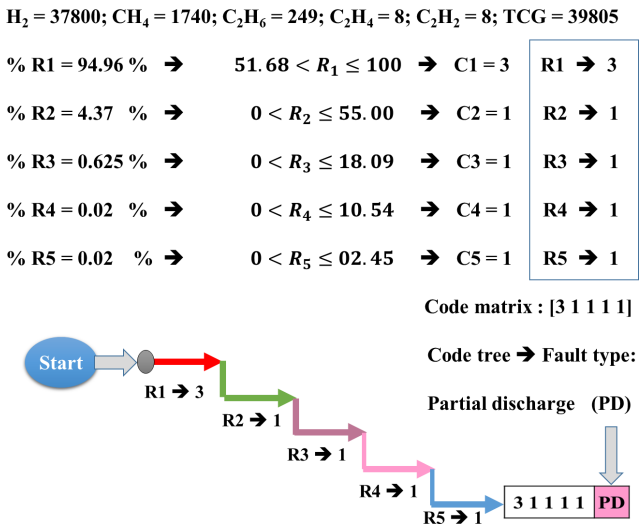

FIGURE 4. Example for using the code tree for fault type estimation.

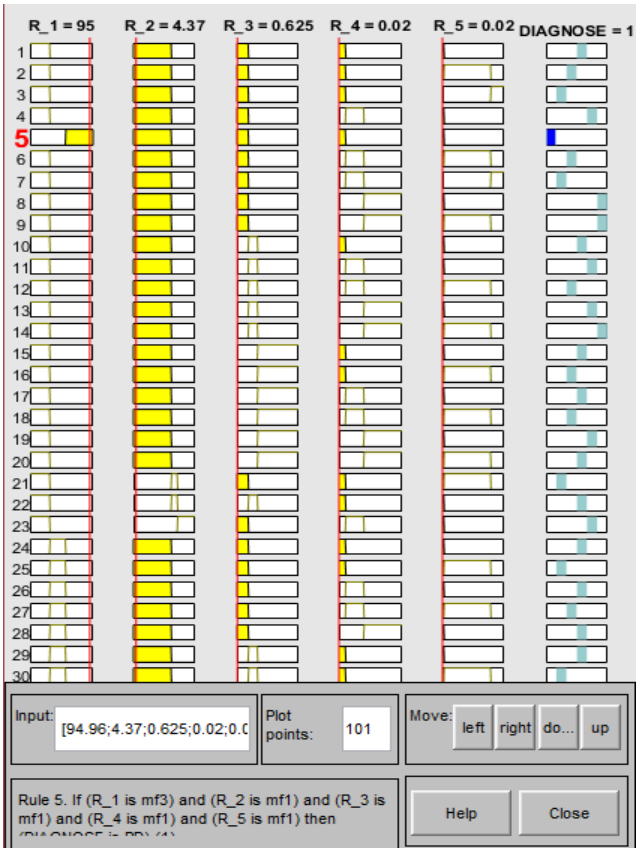

FIGURE 5. Rule viewer of the developed FIS model.

programming or data processing. For further easiness, the developed code tree matrix in Fig. 3 was converted into open access MATLAB code to facilitate the utilizing of the proposed method by engineers at the transformer station. This code was submitted as supplemental material with this paper.

TABLE 4. Sample data for code tree application and fault diagnosis.

Sample number		1	2	3	4	5	6
R1	H_2 (ppm)	37800	124	48	9	109	121
	%	94.96	79.99	22.96	4.327	18.32	699
	code	3	3	1	1	1	1
R2	CH_4 (ppm)	1740	14	20	56	226	450
	%	4.37	9.032	9.57	26.92	37.98	26
	code	1	1	1	1	1	1
R3	C_2H_6 (ppm)	249	4	69	135	68	146
	%	0.625	2.58	33.01	64.9	11.43	8.43
	code	1	1	3	3	1	1
R4	C_2H_4 (ppm)	8	0	41	7	192	898
	%	0.02	0.00065	19.62	3.36	32.27	51.88
	code	1	1	2	1	2	3
R5	C_2H_2 (ppm)	8	13	31	1	0	116
	%	0.02	8.38	14.83	0.48	0	6.70
	code	1	2	2	1	1	2
Code matrix		31111	31112	11322	11311	11121	11132
Proposed diagnosis		PD	D1	D2	T1	T2	T3
Actual diagnosis		PD	D1	D2	T1	T2	T3

VI. RESULTS ANALYSIS AND VALIDATIONS

A. CASE STUDIES

Table 4 illustrates the code matrix formulation for randomly selected five case studies from the original data representing various fault types. The code corresponding to each percentage of dissolved gas concentration was obtained by comparing the values with optimized membership limits in Table 3. Then, the obtained code matrix was used to specify the expected fault type using code tree starting from the center at R1 towards the fault type as described above in Fig. 3. It is clear that the proposed method performs well for the original datasets.

The ability of the proposed code to consider the uncertainties within input data was investigated at different levels. Twelve samples with uncertainty levels of 0%, 5%, 10%, 15% and 20% are considered as study cases. The data samples and corresponding fault types are presented in Table 5. It is clear that the impact of uncertainty in the overall diagnosis was limited. The fault diagnosis using the proposed code tree was correct in all cases except once where the fault changed from T2 to T3 within the same category of thermal fault type.

B. DIAGNOSTIC ACCURACY

Fig. 6 presents the diagnostic accuracy of all fault types during the training stage (1530 data samples) and testing stage (505 data samples) of the original data and uncertain data for all fault types. The results illustrated that the clelosest accuracy for training, testing and overall datasets with overall accuracies of 97.45%, 95.45% and 96.95%, respectively.

TABLE 5. Case studies for fault diagnosis under uncertainty with different levels.

	Sample No.	1		2		3		4		5		6		7		8		9		10		11		12	
	Gas	ppm	%	ppm	%	ppm	%	ppm	%	ppm	%	ppm	%	ppm	%	ppm	%	ppm	%	ppm	%	ppm	%	ppm	%
	H_2	106	93.8	35	6.34	220	30.18	12	8.28	18	11.84	107	21.06	625	90.5	818	39.71	110	16.87	187	41.1	128	8.95	172.9	11.31
	CH_4	4	3.54	6	1.09	77	10.56	28	19.31	63	41.45	143	28.15	49	7.1	94	4.56	62	9.51	86	18.9	419	29.28	334	21.84
	C_2H_6	2	1.77	3	0.54	22	3.02	102	70.34	20	13.16	34	6.69	9	1.3	49	2.38	90	13.8	155	34.07	269.5	18.83	172	11.25
0%	C_2H_4	1	0.88	26	4.71	170	23.32	3	2.07	51	33.55	222	43.7	7	1.01	121	5.87	140	21.47	21	4.62	614.1	42.92	812.5	53.14
	C_2H_2	0	0	482	87.32	240	32.92	0	0	0	0	2	0.39	0.6	0.09	978	47.48	250	38.34	6	1.32	0.35	0.02	37.7	2.47
	ACT	PD		D1		D2		T1		T2		T3		PD		D1		D2		T1		T2		T3	
	Code	**[3 1 1 1 1]**		**[1 1 1 1 3]**		**[1 1 1 2 2]**		**[1 1 3 1 1]**		**[1 1 1 2 1]**		**[1 1 1 3 1]**		**[3 1 1 1 1]**		**[2 1 1 1 2]**		**[1 1 1 2 2]**		**[2 1 3 1 1]**		**[1 1 2 3 1]**		**[1 1 1 3 2]**	
	Diagnose	PD		D1		D2		T1		T2		T3		PD		D1		D2		T1		T2		T3	
	Sample No.	1		2		3		4		5		6		7		8		9		10		11		12	
	Gas	ppm	%	ppm	%	ppm	%	ppm	%	ppm	%	ppm	%	ppm	%	ppm	%	ppm	%	ppm	%	ppm	%	ppm	%
	H_2	104.7	93.71	33.5	6.02	218	29.94	12.19	8.57	17.62	11.4	112.1	22.03	598.8	89.86	853.5	41.66	104.5	16.14	183.8	41.12	134.3	9.31	171.5	11.13
	CH_4	4	3.58	5.83	1.05	77.24	10.61	27.57	19.38	65.97	42.67	138.1	27.16	51.34	7.71	94.4	4.61	59.29	9.15	83.18	18.61	433.2	30.01	328.8	21.35
	C_2H_6	2.05	1.84	3.14	0.56	22.67	3.11	99.39	69.88	20.32	13.14	33	6.51	8.99	1.35	46.59	2.27	93.78	14.48	154.1	34.48	263.3	18.24	166.9	10.83
5%	C_2H_4	0.97	0.87	26.83	4.82	164.8	22.63	3.08	2.16	50.71	32.8	223.3	43.9	6.67	1	115.2	5.62	144.1	22.24	20	4.47	612.2	42.42	834.2	54.15
	C_2H_2	0	0	487.5	87.55	245.5	33.71	0	0	0	0	2	0.39	0.58	0.09	939.1	45.83	246	37.98	5.91	1.32	0.37	0.03	38.98	2.53
	ACT	PD		D1		D2		T1		T2		T3		PD		D1		D2		T1		T2		T3	
	Code	**[3 1 1 1 1]**		**[1 1 1 1 3]**		**[1 1 1 2 2]**		**[1 1 3 1 1]**		**[1 1 1 2 1]**		**[1 1 1 3 1]**		**[3 1 1 1 1]**		**[2 1 1 1 2]**		**[1 1 1 2 2]**		**[2 1 3 1 1]**		**[1 1 2 3 1]**		**[1 1 1 3 2]**	
	Diagnose	PD		D1		D2		T1		T2		T3		PD		D1		D2		T1		T2		T3	
	Sample No.	1		2		3		4		5		6		7		8		9		10		11		12	
	Gas	ppm	%	ppm	%	ppm	%	ppm	%	ppm	%	ppm	%	ppm	%	ppm	%	ppm	%	ppm	%	ppm	%	ppm	%
	H_2	112.4	94.18	32.9	6.37	231.3	31.71	11.19	7.52	16.9	10.46	116.3	22.1	584.2	89.4	897.7	44.02	101.8	15.05	176.7	39.49	139.3	9.8	160.1	10.62
	CH_4	4.21	3.53	6.41	1.24	69.79	9.57	25.98	17.46	67.99	42.06	132.5	25.17	51.5	7.88	84.92	4.16	56.35	8.33	78.95	17.64	386.1	27.16	358.3	23.77
	C_2H_6	1.81	1.52	3.24	0.63	20.58	2.82	108.4	72.84	21.81	13.49	31.89	6.06	9.57	1.46	45.56	2.23	94.52	13.97	165.5	36.98	246.1	17.32	187.7	12.45
10%	C_2H_4	0.92	0.77	27.96	5.42	153.2	21	3.24	2.18	54.95	33.99	243.7	46.32	7.57	1.16	127.7	6.26	151.7	22.42	19.82	4.43	649.5	45.7	767.5	50.9
	C_2H_2	0	0	445.6	86.34	254.6	34.9	0	0	0	0	1.82	0.35	0.63	0.1	883.2	43.31	272.3	40.24	6.52	1.46	0.32	0.02	34.16	2.27
	ACT	PD		D1		D2		T1		T2		T3		PD		D1		D2		T1		T3		T3	
	Code	**[3 1 1 1 1]**		**[1 1 1 1 3]**		**[1 1 1 2 2]**		**[1 1 3 1 1]**		**[1 1 1 2 1]**		**[1 1 1 3 1]**		**[3 1 1 1 1]**		**[2 1 1 1 2]**		**[1 1 1 2 2]**		**[2 1 3 1 1]**		**[1 1 1 3 1]**		**[1 1 1 3 1]**	
	Diagnose	PD		D1		D2		T1		T2		T3		PD		D1		D2		T1		T2		T3	
	Sample No.	1		2		3		4		5		6		7		8		9		10		11		12	
	Gas	ppm	%	ppm	%	ppm	%	ppm	%	ppm	%	ppm	%	ppm	%	ppm	%	ppm	%	ppm	%	ppm	%	ppm	%
	H_2	90.41	93.53	39.86	6.41	242	34.15	10.2	8.15	16.02	10.89	94.84	21.48	554.1	88.61	707.8	33.29	124.5	17.35	212.1	41.53	111.3	7.55	197.5	13.3
	CH_4	3.59	3.71	5.38	0.87	88.13	12.44	24.2	19.32	69.34	47.14	125.5	28.41	54.9	8.78	107.5	5.06	70.74	9.86	97.65	19.13	373.6	25.36	375.6	25.3
	C_2H_6	1.77	1.83	2.67	0.43	19.59	2.76	87.48	69.86	17.27	11.74	30.26	6.85	7.71	1.23	55.31	2.6	80.72	11.25	170.9	33.48	304.1	20.64	148.3	9.99
15%	C_2H_4	0.89	0.92	22.13	3.56	148.1	20.89	3.45	2.67	44.46	30.22	188.8	42.75	7.92	1.27	138	6.49	158.2	22.05	23.34	4.57	684	46.42	721.9	48.62
	C_2H_2	0	0	551.4	88.73	210.8	29.75	0	0	0	0	2.21	0.5	0.68	0.11	1118	52.56	283.2	39.48	6.63	1.3	0.3	0.02	41.49	2.79
	ACT	PD		D1		D2		T1		T2		T3		PD		D1		D2		T1		T2		T3	
	Code	**[3 1 1 1 1]**		**[1 1 1 1 3]**		**[2 1 1 2 2]**		**[1 1 3 1 1]**		**[1 1 1 2 1]**		**[1 1 1 3 1]**		**[3 1 1 1 1]**		**[2 1 1 1 2]**		**[1 1 1 2 2]**		**[2 1 3 1 1]**		**[1 1 2 3 1]**		**[1 1 1 3 2]**	
	Diagnose	PD		D1		D2		T1		T2		T3		PD		D1		D2		T1		T2		T3	
	Sample No.	1		2		3		4		5		6		7		8		9		10		11		12	
	Gas	ppm	%	ppm	%	ppm	%	ppm	%	ppm	%	ppm	%	ppm	%	ppm	%	ppm	%	ppm	%	ppm	%	ppm	%
	H_2	86.79	91.79	29.63	4.74	183	30.07	9.63	5.84	15.02	10.53	88.53	20.55	511.6	90.02	941.6	46.36	88.97	15.82	218.7	48.12	153.1	9.11	138.8	10.65
	CH_4	4.61	4.87	7.08	1.13	63.52	10.44	32.87	19.93	52.75	36.99	115.2	26.74	40.58	7.14	108.9	5.36	49.65	8.83	72.75	16.01	487.4	29	274.9	21.1
	C_2H_6	2.32	2.45	2.48	0.4	25.46	4.19	119.9	72.69	16.14	11.32	40.6	9.42	7.4	1.3	56.96	2.8	103.6	18.43	130.9	28.79	321.1	19.1	203.9	15.65
20%	C_2H_4	0.84	0.88	21.69	3.47	136.1	22.37	2.54	1.54	58.71	41.16	184.2	42.75	8.22	1.45	139.9	6.89	113.6	20.19	25.14	5.53	718.9	42.77	654.4	50.22
	C_2H_2	0	0	564.6	90.27	200.3	32.93	0	0	0	0	2.33	0.54	0.49	0.09	783.8	38.59	206.6	36.73	7.01	1.54	0.28	0.02	31.18	2.39
	ACT	PD		D1		D2		T1		T2		T3		PD		D1		D2		T1		T2		T3	
	Code	**[3 1 1 1 1]**		**[1 1 1 1 3]**		**[1 1 1 2 2]**		**[1 1 3 1 1]**		**[1 1 1 3 1]**		**[1 1 1 3 1]**		**[3 1 1 1 1]**		**[2 1 1 1 2]**		**[1 1 2 2 2]**		**[2 1 3 1 1]**		**[1 1 2 3 1]**		**[1 1 1 3 1]**	
	Diagnose	PD		D1		D2		T1		T3		T3		PD		D1		D2		T1		T3		T3	

The results verified the ability of the proposed code tree to diagnose actual fault types with high accuracy. The accuracy of the proposed method in estimating various fault types for the original dataset without uncertainties was 100%. On the other hand, the ability of the proposed code to specify the fault type considering different degrees of uncertainties is

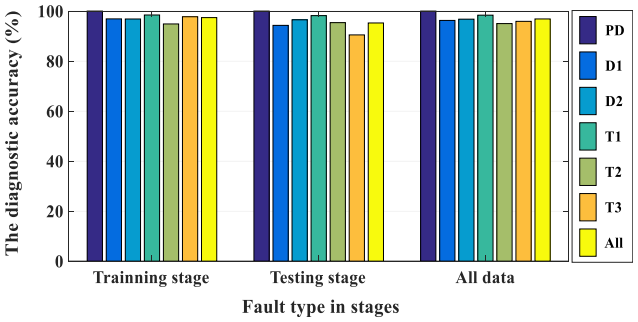

FIGURE 6. Accuracy during the training and testing of all data.

TABLE 6. The diagnostic accuracy of data with 5% uncertainty.

FT	Act	PD	D1	D2	T1	T2	T3	% Accuracy
PD	32	32	0	0	0	0	0	100
D1	59	2	57	0	0	0	0	96.61
D2	99	0	1	98	0	0	0	98.99
T1	86	0	0	0	86	0	0	100
T2	48	0	0	0	0	48	0	100
T3	83	0	0	0	0	2	81	97.59
All	**407**	**34**	**58**	**98**	**86**	**50**	**81**	**98.77**

TABLE 7. The diagnostic accuracy of data with 10% uncertainty.

FT	Act	PD	D1	D2	T1	T2	T3	% Accuracy
PD	32	32	0	0	0	0	0	100
D1	59	0	58	1	0	0	0	98.31
D2	99	0	3	96	0	0	0	96.97
T1	86	0	0	0	86	0	0	100
T2	48	0	0	0	0	47	1	97.92
T3	83	0	0	1	0	2	80	96.39
All	**407**	**32**	**61**	**98**	**86**	**49**	**81**	**98.03**

TABLE 8. The diagnostic accuracy of data with 15% uncertainty.

FT	Act	PD	D1	D2	T1	T2	T3	Accuracy
PD	32	32	0	0	0	0	0	100
D1	59	0	55	4	0	0	0	93.22
D2	99	0	4	94	0	0	1	94.95
T1	86	0	1	0	82	3	0	95.35
T2	48	0	0	0	1	46	1	95.83
T3	83	0	0	1	0	4	78	93.98
All	**407**	**32**	**60**	**99**	**83**	**53**	**80**	**95.09**

TABLE 9. The diagnostic accuracy of data with 20% uncertainty.

FT	Act	PD	D1	D2	T1	T2	T3	Accuracy
PD	32	32	0	0	0	0	0	100
D1	59	1	53	5	0	0	0	89.83
D2	99	0	4	94	0	0	1	94.95
T1	86	1	0	0	84	1	0	97.67
T2	48	0	0	0	1	41	6	85.42
T3	83	0	0	1	0	7	75	90.36
All	**407**	**34**	**57**	**100**	**85**	**49**	**82**	**93.12**

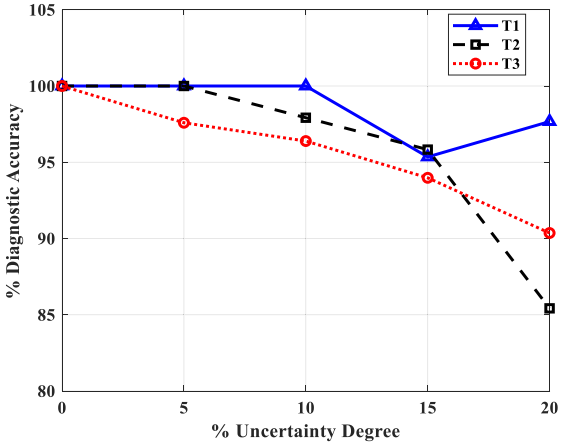

FIGURE 7. Decrement in the diagnostic accuracies against uncertainty degree for thermal faults.

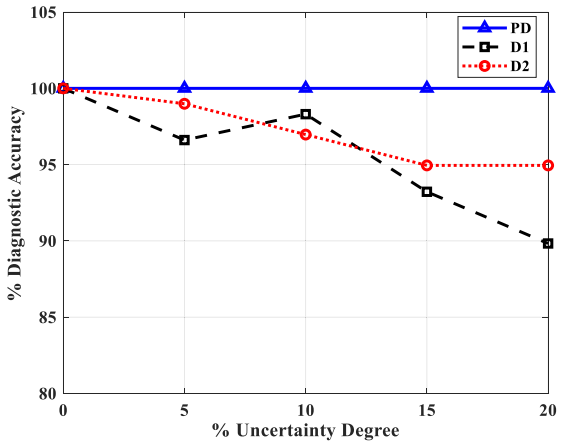

FIGURE 8. Decrement in the diagnostic accuracies against uncertainty degree for discharge faults.

presented in Tables 6, 7, 8 and 9 for 5%, 10%, 15% and 20% uncertainty degree, respectively. The overall diagnostic accuracies are 98.77%, 98.03%, 95.09% and 93.12%, respectively.

The results clarify that the obtained diagnostic accuracies are acceptable and relatively high with respect to the assumed high degree of uncertainties in measurements.

Fig. 7 and Fig. 8 depict the decrement in the diagnostic accuracies for thermal and discharge faults, respectively. The most affected diagnosis by uncertainty occurred for T2 and D1 fault types. The proposed technique proved also robustness against uncertainty above 20%, however this level of uncertainty has not been presented in this study, since it is not common in practice.

It was important to point out that the effect of uncertainty was very limited within the same general group. For example, most of the missing data in D1 fault type were diagnosed as D2 fault which enforces the diagnostic accuracy within

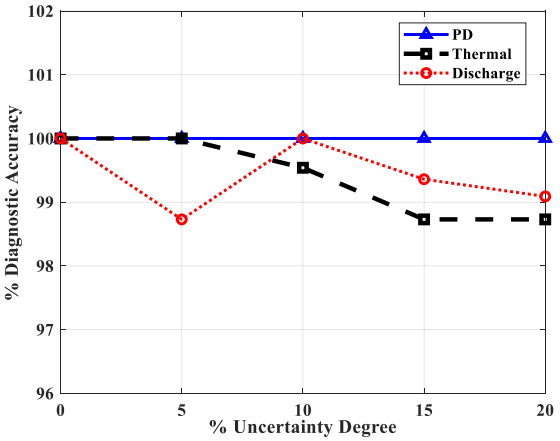

FIGURE 9. Diagnostic accuracy with different uncertainties for different general fault types.

TABLE 10. Comparison of the proposed method with other methods.

% Uncertainty	0%	5%	10%	15%	20%
HGWO	100	98.77	98.03	95.09	93.12
ANN	79.61	78.62	74.45	73.46	72.97
Duval	77.4	76.9	77.15	73.46	72.73
IEC	68.8	68.06	68.06	63.88	63.88
Roger'4 ratio	58.48	58.97	58.72	56.27	56.02
Cluster	84.03	83.05	83.54	78.12	80.1
ROG-MOD	93.86	93.12	91.89	90.17	87.72
IEC-MOD	91.65	90.91	87.96	86.73	88.45

the same category of faults. Fig. 9 presents a summary of the diagnostic accuracies associated with different degree of uncertainties for general groups of faults, partial discharge fault, arcing or discharge fault, and thermal fault. It is clear that the highest decrement in accuracy over the whole uncertainty range was only about 1.3% either for thermal or discharge faults.

C. VALIDATION AND COMPARISON

The ability of the proposed codes to correctly identify the fault type is examined in comparison with other methods. These methods are ANN, Cluster method, IEC ratio method, Duval triangle, modified Rogers'4 ratio (ROG-MOD) [30], and modified IEC ratio [6]. As shown in Table 10, the overall diagnostic accuracy of the proposed method decremented from 100% to 93.12% with a variation of uncertainty from 0% to 20%, which is considered relatively large.

The diagnostic accuracies of the ROG-MOD method (the highest accuracy among the comparison methods) decreased from 93.86% to 87.72% with uncertainty degree varied from 0 to 20%. The accuracy over the whole range of uncertainty degree of the other comparison methods was kept below that of the proposed method. Therefore, the proposed code tree could be used to eliminate the impact of the high degree of uncertainties in measurements.

VII. CONCLUSION

This work had been presented a framework to apply the HGWO optimizer technique in order to generate a new code matrix for the power transformer fault diagnosis considering the uncertainty associated with the measurements. The GWO optimizer was modified by adding two loops of PSO and GA to improve the ability to divert and converge at the optimal solution. GA and PSO was additionally used separately to guarantee obtaining the global optimal solution. The uncertainty in the measured data that originated either during oil sampling or during storage and transfer were considered up to 20% of the actual measured data.

The developed code matrix succeeded to diagnose the fault types with a high accuracy of 100% for the original dataset as well as 98.77%, 98.03%, 95.09% and 93.12% in the case of random uncertainty of 5%, 10%, 15% and 20%, respectively. The proposed code matrix had high abilities to diagnose the transformer fault types using simple codes and with high degree of uncertainties in the measurements. The comparison between the proposed code matrix and other DGA methods such as ANN, Duval, IEC 60599 Code, Cluster, ROG-MOD and IEC-MOD methods proved its effectiveness and applicability in accurate fault diagnosis considering uncertainties. The accuracies of the proposed code over the whole range of uncertainty degree were higher than that of other methods.

REFERENCES

[1] *IEEE Guide for the Interpretation of Gases Generated in Mineral Oil-Immersed Transformers*, IEEE Standard C57.104-2008, Feb. 2009.

[2] J. Singh, Y. R. Sood, and P. Verma, "The influence of service aging on transformer insulating oil parameters," *IEEE Trans. Dielectr. Electr. Insul.*, vol. 19, no. 2, pp. 421–426, Apr. 2012.

[3] H. Zheng, Y. Zhang, J. Liu, H. Wei, J. Zhao, and R. Liao, "A novel model based on wavelet LS-SVM integrated improved PSO algorithm for forecasting of dissolved gas contents in power transformers," *Electr. Power Syst. Res.*, vol. 155, pp. 196–205, Feb. 2018.

[4] M. E. A. Senoussaoui, M. Brahami, and I. Fofana, "Combining and comparing various machine-learning algorithms to improve dissolved gas analysis interpretation," *IET Gener., Transmiss. Distrib.*, vol. 12, no. 15, pp. 3673–3679, Aug. 2018.

[5] J. Li, Q. Zhang, K. Wang, J. Wang, T. Zhou, and Y. Zhang, "Optimal dissolved gas ratios selected by genetic algorithm for power transformer fault diagnosis based on support vector machine," *IEEE Trans. Dielectr. Electr. Insul.*, vol. 23, no. 2, pp. 1198–1206, Apr. 2016.

[6] S. I. Ibrahim, S. S. M. Ghoneim, and I. B. M. Taha, "DGALab: An extensible software implementation for DGA," *IET Gener., Transmiss. Distrib.*, vol. 12, no. 18, pp. 4117–4124, Oct. 2018.

[7] O. E. Gouda, S. H. El-Hoshy, and H. H. E. L. Tamaly, "Proposed three ratios technique for the interpretation of mineral oil transformers based dissolved gas analysis," *IET Gener., Transmiss. Distrib.*, vol. 12, no. 11, pp. 2650–2661, Jun. 2018.

[8] M. Duval, "A review of faults detectable by gas-in-oil analysis in transformers," *IEEE Elect. Insul. Mag.*, vol. 18, no. 3, pp. 8–17, May 2002.

[9] D. A. Mansour, "A new graphical technique for the interpretation of dissolved gas analysis in power transformers," in *Proc. Annu. Rep. Conf. Electr. Insul. Dielectric Phenomena*, Montreal, QC, Canada, Oct. 2012, pp. 195–198.

[10] M. Duval and L. Lamarre, "The duval pentagon—A new complementary tool for the interpretation of dissolved gas analysis in transformers," *IEEE Electr. Insul. Mag.*, vol. 30, no. 6, pp. 9–12, Nov. 2014.

[11] C. Xiang, Z. Huang, J. Li, Q. Zhou, and W. Yao, "Graphic approaches for faults diagnosis for Camellia insulating liquid filled transformers based on dissolved gas analysis," *IEEE Trans. Dielectr. Electr. Insul.*, vol. 25, no. 5, pp. 1897–1903, Oct. 2018.
[12] O. E. Gouda, S. H. El-Hoshy, and H. H. El-Tamaly, "Proposed heptagon graph for DGA interpretation of oil transformers," *IET Gener., Transmiss. Distrib.*, vol. 12, no. 2, pp. 490–498, Jan. 2018.
[13] M. A. Izzularab, G. E. M. Aly, and D. A. Mansour, "On-line diagnosis of incipient faults and cellulose degradation based on artificial intelligence methods," in *Proc. IEEE Int. Conf. Solid Dielectr.*, Toulouse, France, Jul. 2004, pp. 767–770.
[14] V. Miranda and A. R. G. Castro, "Improving the IEC table for transformer failure diagnosis with knowledge extraction from neural networks," *IEEE Trans. Power Del.*, vol. 20, no. 4, pp. 2509–2516, Oct. 2005.
[15] S. Souahlia, K. Bacha, and A. Chaari, "MLP neural network-based decision for power transformers fault diagnosis using an improved combination of Rogers and Doernenburg ratios DGA," *Int. J. Electr. Power Energy Syst.*, vol. 43, no. 1, pp. 1346–1353, Dec. 2012.
[16] S. S. M. Ghoneim, I. B. M. Taha, and N. I. Elkalashy, "Integrated ANN-based proactive fault diagnostic scheme for power transformers using dissolved gas analysis," *IEEE Trans. Dielectr. Electr. Insul.*, vol. 23, no. 3, pp. 1838–1845, Jun. 2016.
[17] S. A. Wani, D. Gupta, M. U. Farooque, and S. A. Khan, "Multiple incipient fault classification approach for enhancing the accuracy of dissolved gas analysis (DGA)," *IET Sci., Meas. Technol.*, vol. 13, no. 7, pp. 959–967, Sep. 2019.
[18] I. B. M. Taha, S. S. M. Ghoneim, and H. G. Zaini, "A fuzzy diagnostic system for incipient transformer faults based on DGA of the insulating transformer oils," *Int. Rev. Electr. Eng.*, vol. 11, no. 3, pp. 305–313, Jul. 2016.
[19] Y.-C. Huang and H.-C. Sun, "Dissolved gas analysis of mineral oil for power transformer fault diagnosis using fuzzy logic," *IEEE Trans. Dielectr. Electr. Insul.*, vol. 20, no. 3, pp. 974–981, Jun. 2013.
[20] A. Abu-Siada, S. Hmood, and S. Islam, "A new fuzzy logic approach for consistent interpretation of dissolved gas-in-oil analysis," *IEEE Trans. Dielectr. Electr. Insul.*, vol. 20, no. 6, pp. 2343–2349, Dec. 2013.
[21] Y. Zhang, X. Li, H. Zheng, H. Yao, J. Liu, C. Zhang, H. Peng, and J. Jiao, "A fault diagnosis model of power transformers based on dissolved gas analysis features selection and improved krill herd algorithm optimized support vector machine," *IEEE Access*, vol. 7, pp. 102803–102811, 2019.
[22] V. Tra, B.-P. Duong, and J.-M. Kim, "Improving diagnostic performance of a power transformer using an adaptive over-sampling method for imbalanced data," *IEEE Trans. Dielectr. Electr. Insul.*, vol. 26, no. 4, pp. 1325–1333, Aug. 2019.
[23] K. Bacha, S. Souahlia, and M. Gossa, "Power transformer fault diagnosis based on dissolved gas analysis by support vector machine," *Electr. Power Syst. Res.*, vol. 83, no. 1, pp. 73–79, Feb. 2012.
[24] T. Kari, W. Gao, D. Zhao, Z. Zhang, W. Mo, Y. Wang, and L. Luan, "An integrated method of ANFIS and Dempster-Shafer theory for fault diagnosis of power transformer," *IEEE Trans. Dielectr. Electr. Insul.*, vol. 25, no. 1, pp. 360–371, Feb. 2018.
[25] H. Malik and S. Mishra, "Application of gene expression programming (GEP) in power transformers fault diagnosis using DGA," *IEEE Trans. Ind. Appl.*, vol. 52, no. 6, pp. 4556–4565, Nov. 2016.
[26] J. I. Aizpurua, V. M. Catterson, B. G. Stewart, S. D. J. McArthur, B. Lambert, B. Ampofo, G. Pereira, and J. G. Cross, "Power transformer dissolved gas analysis through Bayesian networks and hypothesis testing," *IEEE Trans. Dielectr. Electr. Insul.*, vol. 25, no. 2, pp. 494–506, Apr. 2018.
[27] H. Ma, C. Ekanayake, and T. K. Saha, "Power transformer fault diagnosis under measurement originated uncertainties," *IEEE Trans. Dielectr. Electr. Insul.*, vol. 19, no. 6, pp. 1982–1990, Dec. 2012.
[28] M. Duval and A. dePabla, "Interpretation of gas-in-oil analysis using new IEC publication 60599 and IEC TC 10 databases," *IEEE Elect. Insul. Mag.*, vol. 17, no. 2, pp. 31–41, Mar. 2001.
[29] *Dissolved Gas Analysis Reports*, Egyptian Electr. Holding Company, Cairo, Egypt, 2016.
[30] I. B. M. Taha, A. Hoballah, and S. S. M. Ghoneim, "Optimal ratio limits of Rogers' four-ratios and IEC 60599 code methods using particle swarm optimization fuzzy-logic approach," *IEEE Trans. Dielectr. Electr. Insul.*, vol. 27, no. 1, pp. 222–230, Feb. 2020.
[31] E. Li, L. Wang, and B. Song, "Fault diagnosis of power transformers with membership degree," *IEEE Access*, vol. 7, pp. 28791–28798, Feb. 2019.
[32] S. M. Korobeynikov, A. V. Ridel, A. Y. Korobenkova, and D. V. Vagin, "Dissolution of bubbles with diagnostic gases in insulating liquids," in *Proc. IEEE 19th Int. Conf. Dielectr. Liquids (ICDL)*, Manchester, U.K., Jun. 2017, pp. 1–4.
[33] S. Tenbohlen, J. Aragon-Patil, M. Fischer, M. Schäfer, Z. D. Wang, and I. H. Atanasova, "Investigation on sampling, measurement and interpretation of gas-in-oil analysis for power transformers," in *Proc. CIGRE*, 2008, p. D1-204.
[34] S. A. Khan, M. D. Equbal, and T. Islam, "A comprehensive comparative study of DGA based transformer fault diagnosis using fuzzy logic and ANFIS models," *IEEE Trans. Dielectr. Electr. Insul.*, vol. 22, no. 1, pp. 590–596, Feb. 2015.
[35] R. Naresh, V. Sharma, and M. Vashisth, "An integrated neural fuzzy approach for fault diagnosis of transformers," *IEEE Trans. Power Del.*, vol. 23, no. 4, pp. 2017–2024, Oct. 2008.
[36] V. Miranda, A. R. G. Castro, and S. Lima, "Diagnosing faults in power transformers with autoassociative neural networks and mean shift," *IEEE Trans. Power Del.*, vol. 27, no. 3, pp. 1350–1357, Jul. 2012.
[37] I. B. M. Taha, D. A. Mansour, S. S. M. Ghoneim, and N. I. Elkalashy, "Conditional probability-based interpretation of dissolved gas analysis for transformer incipient faults," *IET Gener., Transmiss. Distrib.*, vol. 11, no. 4, pp. 943–951, Mar. 2017.
[38] S. Mirjalili, S. M. Mirjalili, and A. Lewis, "Grey wolf optimizer," *Adv. Eng. Softw.*, vol. 69, pp. 46–61, Mar. 2014.
[39] M. A. Tawhid and A. F. Ali, "A hybrid grey wolf optimizer and genetic algorithm for minimizing potential energy function," *Memetic Comput.*, vol. 9, no. 4, pp. 347–359, May 2017.
[40] J. Faiz and M. Soleimani, "Assessment of computational intelligence and conventional dissolved gas analysis methods for transformer fault diagnosis," *IEEE Trans. Dielectr. Electr. Insul.*, vol. 25, no. 5, pp. 1798–1806, Oct. 2018.
[41] T. Kari, W. Gao, D. Zhao, K. Abiderexiti, W. Mo, Y. Wang, and L. Luan, "Hybrid feature selection approach for power transformer fault diagnosis based on support vector machine and genetic algorithm," *IET Gener., Transmiss. Distrib.*, vol. 12, no. 21, pp. 5672–5680, Nov. 2018.
[42] S. Arora, H. Singh, M. Sharma, S. Sharma, and P. Anand, "A new hybrid algorithm based on grey wolf optimization and crow search algorithm for unconstrained function optimization and feature selection," *IEEE Access*, vol. 7, pp. 26343–26361, 2019.
[43] H. Y. Mahmoud, H. M. Hasanien, A. H. Besheer, and A. Y. Abdelaziz, "Hybrid cuckoo search algorithm and grey wolf optimiser-based optimal control strategy for performance enhancement of HVDC-based offshore wind farms," *IET Gener., Transmiss. Distrib.*, vol. 14, no. 10, pp. 1902–1911, May 2020.
[44] B. Zeng, J. Guo, W. Zhu, Z. Xiao, F. Yuan, and S. Huang, "A transformer fault diagnosis model based on hybrid grey wolf optimizer and LS-SVM," *Energies*, vol. 12, no. 21, Nov. 2019, Art. no. 4170.
[45] Q. Al-Tashi, S. J. Abdul Kadir, H. M. Rais, S. Mirjalili, and H. Alhussian, "Binary optimization using hybrid grey wolf optimization for feature selection," *IEEE Access*, vol. 7, pp. 39496–39508, 2019.

AYMAN HOBALLAH received the B.Sc. and M.Sc. degrees in electrical engineering from Tanta University, Egypt, in 1996 and 2003, respectively, and the Ph.D. degree from the Electrical Engineering Department, University of Duisburg-Essen, Germany, in 2011. His Ph.D. thesis focuses on the power system dynamic stability, enhancement utilizing artificial intelligent techniques. Since 1998, he has been with the Electrical Power and Machines Department, Faculty of Engineering, Tanta University. He is currently an Associate Professor with Taif University. His current research interests include power system stability, DGs, smart grid, grounding systems, and optimization techniques.

DIAA-ELDIN A. MANSOUR (Senior Member, IEEE) was born in Tanta, Egypt, in December 1978. He received the B.Sc. and M.Sc. degrees in electrical engineering from Tanta University, Tanta, Egypt, in 2000 and 2004, respectively, and the Ph.D. degree in electrical engineering from Nagoya University, Nagoya, Japan, in 2010. Since 2000, he has been with the Department of Electrical Power and Machines Engineering, Faculty of Engineering, Tanta University, as an Instructor and an Assistant Lecturer. In 2010, he was a Foreign Researcher with the Eco Topia Science Institute, Nagoya University, for a period of three months. He is currently an Assistant Professor and the Director of the High Voltage and Superconductivity Laboratory, Tanta University. His research interests include high-voltage engineering, condition monitoring and diagnosis of electrical power equipment, nanodielectrics, and renewable energy systems. He received the Best Presentation Award two times from the IEE of Japan, in 2008 and 2009, the Prof. Khalifa's Prize from the Egyptian Academy of Scientific Research and Technology, in 2013, the Tanta University Encouragement Award, in 2017, and the State Encouragement Award, in 2018.

IBRAHIM B. M. TAHA received the B.Sc. degree from the Faculty of Engineering, Tanta University, Tanta, Egypt, in 1995, the M.Sc. degree from the Faculty of Engineering, Mansoura University, Mansoura, Egypt, in 1999, and the Ph.D. degree in electrical power and machines from the Faculty of Engineering, Tanta University, in 2007. In 1996, he was a Teaching Staff with the Faculty of Engineering, Tanta University. He is currently an Assistant Professor and an Associate Professor with the Electrical Engineering Department, Faculty of Engineering. Taif University. His research interests include steady state and transient stability of HVDC systems, FACTS, load forecasting, multi-level inverters, dissolved gas analysis, and artificial intelligent technique applications.